ChemComm

RSC Publishing

COMMUNICATION

View Article Online
View Journal | View Issue

Published on 14 May 2013. Downloaded by Michigan State University on 20/01/2016 09:48:36.

Cite this: *Chem. Commun.*, 2013, **49**, 5981

Received 22nd March 2013,
Accepted 14th May 2013

DOI: 10.1039/c3cc42109k

www.rsc.org/chemcomm

One-pot galvanic formation of ultrathin-shell Sn/CoO_x nanohollows as high performance anode materials in lithium ion batteries†

Juan Xu,[a] Jaewon Jin,[a] Kyeongyeol Kim,[a] Young Jun Shin,[a] Hae Jin Kim[b] and Seung Uk Son*[a]

The thermolysis of a heterobimetallic Sn–Co organometallic precursor resulted in the formation of hollow Sn/CoO_x nanomaterials through galvanic reaction between metal species. The Sn/CoO_x nanohollows with 6.1 nm diameter and ~1.5 nm shell thickness showed excellent lithium storage capacity of up to 857 mA h g^{-1} after 30 cycles.

The chemical activities of nanomaterials are closely related to their size and surface area.[1] In addition, the shape effect of nanomaterials can be critical in their chemical functions.[2] For example, various inorganic nanomaterials have been applied as energy storage materials in lithium ion batteries.[3] For evaluating the electrochemical performance of electrode materials, the energy storage capacity and stability are important parameters. To enhance the energy storage capacity, the size of electrode materials has been controlled to sub-10 nm. The shape of electrode materials is related to their electrochemical stability. The existence of inner empty space in materials enhances the stability of their electrochemical functions because it enables the electrode materials to maintain their functions against volume change after lithium insertion.[3b] In this regard, various hollow nanomaterials have been prepared to achieve high capacity and stability as electrode materials in lithium ion batteries.[4]

Group IVA elements are extensively used as anode materials in lithium ion batteries.[5] Their electrochemical performances are based on the alloying and de-alloying processes triggered by lithium insertion and desertion. Among the group IVA elements, tin-containing nanomaterials have been most widely prepared.[4,6–8] Zerovalent tin can be used as an anode material in lithium ion batteries.[7,8] However, the size of zerovalent tin materials reported thus far has been relatively large (>10 nm), due to the limited synthetic routes, especially for sub 3 nm-sized materials.[7,8] Moreover, hollow zerovalent tin materials are quite rare.[8]

A single-precursor approach for the preparation of nanomaterials is attractive because the synthetic steps can be simplified.[9] For the synthesis of multi-component materials, precursors having the corresponding multi-elements have been prepared.[9] Usually, single precursors with a tailored stoichiometry of elements have been used for the selective control of target stoichiometric phases. In comparison, as far as we are aware, the use of multi-component single precursors for the shape-controlled synthesis of nanomaterials has not been reported. Our research group has studied the shape-controlled synthesis of functional nanomaterials.[10] In this work, we report the synthesis of tin containing hollow nanomaterials with ultrathin shells using a multi-component single precursor and their performance as an anode material in lithium ion batteries.

As shown in Fig. 1, a heterobimetallic precursor with tin and cobalt was prepared.[11] Originally, this precursor was designed for the preparation of Sn–Co hetero-component anode materials because both Sn and cobalt oxide are active as anode materials.[3b] First, to confer nucleophilicity on cobalt, $Co_2(CO)_8$ was reduced to Co(−1) species using sodium naphthalenide. The resultant $NaCo(CO)_4$ was reacted with a tin electrophile (Ph_3SnCl) to form the target precursor, $Ph_3SnCo(CO)_4$. Its elemental analysis (theoretical values for C: 50.72 and H: 2.90, observed values for C: 50.78 and H: 2.96) confirmed the high purity of the obtained precursor. For the synthesis of ultrathin Sn/CoO_x hollow nanospheres (**US-HS**),

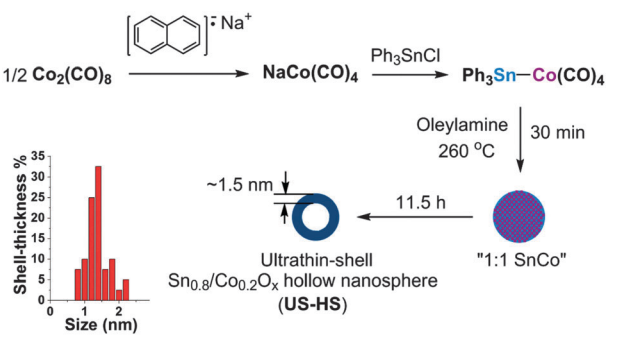

Fig. 1 Synthesis of a Sn–Co heterobimetallic precursor and ultrathin-shell Sn/CoO_x hollow nanospheres (**US-HS**).

[a] *Department of Chemistry and Department of Energy Science, Sungkyunkwan University, Suwon 440-746, Korea. E-mail: sson@skku.edu; Fax: +82-031-290-4572*

[b] *Korea Basic Science Institute, Daejeon 350-333, Korea*

† Electronic supplementary information (ESI) available: Experimental details, HR-TEM image and cyclovoltammogram of an electrochemical cell. See DOI: 10.1039/c3cc42109k

Published on 14 May 2013. Downloaded by Michigan State University on 20/01/2016 09:48:36.

the Sn–Co heterobimetallic precursor was dissolved in well-dried oleylamine and injected into a hot oleylamine solution at 260 °C. The reaction mixture was heated for additional 12 hours. After cooling to room temperature, excess methanol was added to form precipitates which were retrieved by centrifugation (refer to the ESI† for details).

Transmission electron microscopy (TEM) analysis of the obtained materials showed nanospheres with empty inner space (Fig. 2). The average size of materials was 6.1 ± 0.5 nm with a shell thickness of ~1.5 ± 0.3 nm (Fig. 1 and Fig. S1 in the ESI†).[12] To elucidate the formation mechanism of the hollow nanospheres, the materials formed at different reaction times were analyzed using energy dispersive X-ray spectroscopy (EDS), powder X-ray diffraction studies (PXRD), TEM and X-ray photoelectron microscopy (XPS) (Fig. 3).

The materials formed after 30 min showed nearly a 1 : 1 stoichiometric ratio of tin to cobalt in EDS analysis. As time passed, the cobalt content gradually decreased to 0.2 eq. to tin after 12 hours (Fig. 3a). According to PXRD studies, the powders obtained after 30 min and 1 hour showed amorphous character (Fig. 3b). Interestingly, PXRD peaks corresponding to zerovalent tin (JCPDS# 86-2265) appeared after 12 hours. In the XPS analysis of the materials obtained after 30 min and 12 hours, the $2p_{3/2}$ orbital peak of cobalt shifted from 778.3 eV to a higher energy level of 780.0 eV (Fig. 3c). The peaks at 778.3 eV and 780.0 eV were close to those of zerovalent Co and Co(+2), respectively.[13] In contrast, the $3d_{5/2}$ orbital peak of tin shifted from 486.4 eV to a lower energy level of 485.4 eV. The peaks at 486.4 eV and 485.4 eV were close to Sn(+2) and zerovalent Sn, respectively.[13] Thus, as the reaction proceeded after 30 min, cobalt was oxidized to cobalt(+2) ions and at the same time, tin(+2) was reduced to zerovalent tin. Considering the standard reduction potentials of cobalt(+2) and tin(+2) ions, a redox reaction between cobalt and tin species is thermodynamically reasonable.[14] TEM analysis of the materials obtained after 30 min and 12 hours showed ~7 nm-sized spheres (Fig. 3d) and hollow spheres with ~6 nm diameter (Fig. 3e).

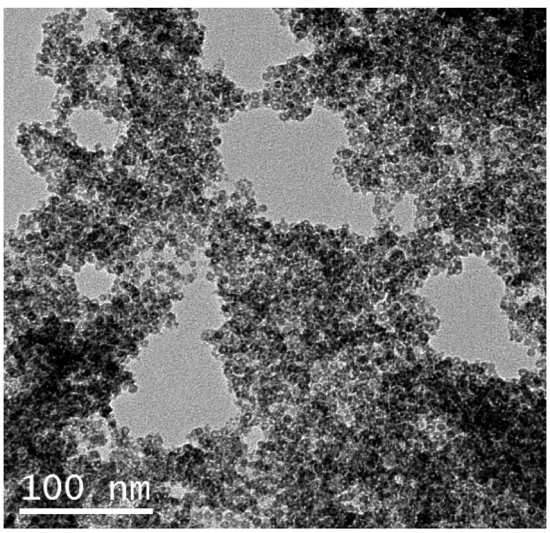

Fig. 2 TEM image of ultrathin-shell Sn/CoO_x hollow nanospheres (**US-HS**). Also refer to the magnified image in the ESI† (Fig. S2).

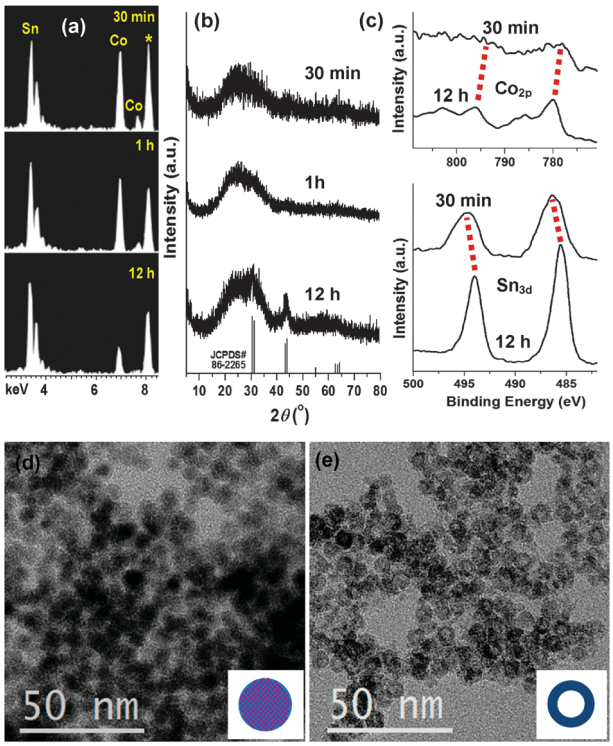

Fig. 3 (a) EDS (* = Cu from grid) and (b) PXRD studies of the materials obtained after heating $Ph_3SnCo(CO)_4$ in oleylamine at 260 °C for 30 min, 1 h and 12 hours. (c) XPS and TEM analysis (also, refer to Fig. S4 in the ESI†) of the materials obtained after 30 min (d) and 12 hours (e).

High-resolution TEM studies on the hollows showed poor crystallinity due to the size effect (Fig. S3, ESI†). After 18 hours, the hollow structures collapsed. Thus, it can be speculated that cobalt was gradually removed from the materials *via* oxidation and zerovalent tin gradually formed in the hollows with inner empty space.

Next, we investigated the electrochemical properties of **US-HS** as an anode material in lithium ion batteries. Using **US-HS**, working electrodes were fabricated (see the ESI† for detailed procedures). Then, coin-type electrochemical cells were assembled using lithium metal as a counter electrode. The cells were discharged from open voltage and cycled between 1 mV and 2 V with a current density of 50 mA g^{-1}. It has been reported that metallic tin acts as an anode material through reversible lithiation and de-lithiation to form a $Li_{4.4}Sn$ alloy.[7,8] In addition, CoO is active as an anode material.[3b] **US-HS** showed the typical cyclovoltammogram of tin-based anode materials (Fig. S4, ESI†). The redox reaction at +0.8 V (*vs.* Li/Li^+) by CoO can be overlapped (Fig. S5 in the ESI†). Fig. 4a shows the cycling performance of the cell of **US-HS**. The theoretical maximum storage capacity of metallic tin is known to be 992 mA h g^{-1}.[7,8] The first discharge capacity of the cell of **US-HS** was observed to be 2530 mA h g^{-1}, which originated from both irreversible and reversible electrochemical processes. It has been suggested in the literature that this irreversible process in the early stages of tin anode materials is related to the formation of a solid electrolyte interface (SEI).[7,8] The relatively large irreversible capacity in the first cycle originated from the size effect of materials. The discharge capacities were gradually stabilized in successive runs. After 30 cycles, the electrochemical cells

 This journal is © The Royal Society of Chemistry 2013

Published on 14 May 2013. Downloaded by Michigan State University on 20/01/2016 09:48:36.

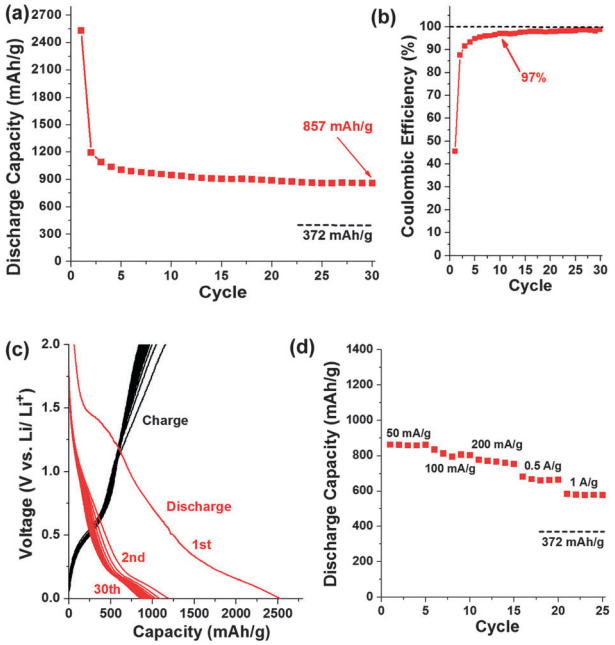

Fig. 4 (a) Cycling performance, (b) coulombic efficiencies, (c) charge–discharge curves with a 50 mA g^{-1} current density and (d) current density-dependent discharge capacities of the electrochemical cells prepared using **US-HS**.

maintained a discharge capacity of 857 mA h g^{-1} (based on the weight of **US-HS**), which corresponds to 86% and 91% of the theoretical maximum capacity of zerovalent tin and $Sn_{0.8}/(CoO)_{0.2}$ anode materials respectively.[3b,15] Notably, in the last five cycles, the change in discharge capacity was only within 3 mA h g^{-1}. In the literature, the sizes of zerovalent tin-based anode materials were in the range of 10–100 nm.[7,8] The lithium storage capacities were observed to be in the range of 500–800 mA h g^{-1}.[7,8] Considering these values, it can be speculated that the high capacity of electrochemical cells of **US-HS** and the stability are attributed to the sub 10 nm size and hollow structure.[16] Especially, it is noteworthy that the Li diffusion length corresponds to the shell thickness of **US-HS**, which is ~1.5 nm.

As shown in Fig. 4b, the coulombic efficiencies sharply increased from 46% to 97% in the first 10 cycles and maintained the higher values in successive runs. The charge–discharge curves showed typical patterns of electrochemical cells based on the tin alloying–de-alloying process (Fig. 4c).[7,8] The shoulder peak in the ~1–1.5 V range in the first discharge curve is typically assigned to the irreversible decomposition of the electrolyte or the formation of SEI.[7,8] The voltages below 1 V in Fig. 4c correspond to the reversible delithiation–lithiation, and match well with the conventional behavior of tin-based anode materials.[7,8] The electrochemical cells maintained good performance at higher current densities (Fig. 4d). At current densities of 100 mA g^{-1} and 200 mA g^{-1}, the cells maintained discharge capacities of 802 mA h g^{-1} and 770 mA h g^{-1}, corresponding to 81% and 78% of the theoretical maximum capacity, respectively. Even with current densities of 0.5 A g^{-1} and 1 A g^{-1}, the cells showed discharge capacities of 663 mA h g^{-1} and 578 mA h g^{-1}, which are 67% and 58% of the theoretical maximum capacity of tin, respectively, and much higher than that of commercialized graphite (372 mA h g^{-1}).

In conclusion, in this work we have shown that ultrathin-shell hollow nanomaterials can be prepared in a one-pot process through an organometallic single-precursor approach. We believe that more diverse nano-structured materials can be prepared in one-pot by the delicate design of single precursors with multi-elements with different electrochemical properties.

This work was supported by grants NRF-2012-004029 (Basic Science Research Program) through the National Research Foundation of Korea funded by the MEST. JX thanks for grants NRF-2012-1040282 (Priority Research Centers Program) and R31-2008-10029 (WCU program).

Notes and references

1 Review: X. Chen, C. Li, M. Grätzel, R. Kostecki and S. S. Mao, *Chem. Soc. Rev.*, 2012, **41**, 7909.
2 Recent review: Z.-Y. Zhou, N. Tian, J.-T. Li, I. Broadwell and S.-G. Sun, *Chem. Soc. Rev.*, 2011, **40**, 4167.
3 (*a*) H. B. Wu, J. S. Chen, H. H. Hng and X. W. Lou, *Nanoscale*, 2012, **4**, 2526; (*b*) P. Poizot, S. Laruelle, S. Grugeon, L. Dupont and J.-M. Tarascon, *Nature*, 2000, **407**, 496.
4 Recent review: J. S. Chen, L. A. Archer and X. W. Lou, *J. Mater. Chem.*, 2011, **21**, 9912.
5 Reviews: (*a*) L. Ji, Z. Lin, M. Alcoutlabi and X. Zhang, *Energy Environ. Sci.*, 2011, **4**, 2682; (*b*) N.-S. Choi, Y. Yao, Y. Cui and J. Cho, *J. Mater. Chem.*, 2011, **21**, 9825; selected examples: (*c*) A. M. Chockla, J. T. Harris, V. A. Akhavan, T. D. Bogart, V. C. Holmberg, C. Steinhagen, C. B. Mullins, K. J. Stevenson and B. A. Korgel, *J. Am. Chem. Soc.*, 2011, **133**, 20914; (*d*) L. Xue, G. Xu, Y. Li, S. Li, K. Fu, Q. Shi and X. Zhang, *ACS Appl. Mater. Interfaces*, 2013, **5**, 21.
6 Selected examples: (*a*) X. W. Lou, Y. Wang, C. Yuan, J. Y. Lee and L. A. Archer, *Adv. Mater.*, 2006, **18**, 2325; (*b*) S. Ding and X. W. Lou, *Nanoscale*, 2011, **3**, 3586; (*c*) Y. Chen, Q. Z. Huang, J. Wang, Q. Wang and J. M. Xue, *J. Mater. Chem.*, 2011, **21**, 17448; (*d*) M. Zhang, D. Lei, X. Yu, L. Chen, Q. Li, Y. Wang, T. Wang and G. Cao, *J. Mater. Chem.*, 2012, **22**, 23091.
7 Selected examples: (*a*) C.-C. Chang, S.-J. Liu, J.-J. Wu and C.-H. Yang, *J. Phys. Chem. C*, 2007, **111**, 16423; (*b*) W.-M. Zhang, J.-S. Hu, Y.-G. Guo, S.-F. Zheng, L.-S. Zhong, W.-G. Song and L.-J. Wan, *Adv. Mater.*, 2008, **20**, 1160; (*c*) G. Wang, B. Wang, X. Wang, J. Park, S. Dou, H. Ahn and K. Kim, *J. Mater. Chem.*, 2009, **19**, 8378; (*d*) Y. Yu, L. Gu, C. Zhu, P. A. van Aken and J. Maier, *J. Am. Chem. Soc.*, 2009, **131**, 15984; (*e*) K.-C. Hsu, C.-E. Liu, P.-C. Chen, C.-Y. Lee and H.-T. Chiu, *J. Mater. Chem.*, 2012, **22**, 21533.
8 G. Cui, Y.-S. Hu, L. Zhi, D. Wu, I. Lieberwirth, J. Maier and K. Müllen, *Small*, 2007, **3**, 2066.
9 Selected examples: (*a*) J. Xu, K. Jang, J. Lee, H. J. Kim, J. Jeong, J.-G. Park and S. U. Son, *Cryst. Growth Des.*, 2011, **11**, 2707; (*b*) K. Jang, I.-Y. Lee, J. Xu, J. Choi, J. Jin, J. H. Park, H. J. Kim, G.-H. Kim and S. U. Son, *Cryst. Growth Des.*, 2012, **12**, 3388.
10 (*a*) K. H. Park, K. Jang and S. U. Son, *Angew. Chem., Int. Ed.*, 2006, **45**, 4608; (*b*) K. H. Park, K. Jang and S. U. Son, *Angew. Chem., Int. Ed.*, 2007, **46**, 1152; (*c*) K. H. Park, J. Choi, H. J. Kim, J. R. Ahn and S. U. Son, *Small*, 2008, **4**, 945; (*d*) K. H. Park, J. Choi, H. J. Kim, J. B. Lee and S. U. Son, *Chem. Mater.*, 2007, **19**, 3861; (*e*) J. Xu, K. Jang, I. G. Jung, H. J. Kim, D.-H. Oh, J. R. Ahn and S. U. Son, *Chem. Mater.*, 2009, **21**, 4347; (*f*) J. Choi, N. Kang, H. Y. Yang, H. J. Kim and S. U. Son, *Chem. Mater.*, 2010, **22**, 3586; (*g*) J. Choi, J. Jin, I. G. Jung, J. M. Kim, H. J. Kim and S. U. Son, *Chem. Commun.*, 2011, **47**, 5241; (*h*) J. Xu, K. Jang, J. Choi, J. Jin, J. H. Park, H. J. Kim, D.-H. Oh, J. R. Ahn and S. U. Son, *Chem. Commun.*, 2012, **48**, 6244.
11 A. D. Beveridge and H. C. Clark, *J. Organomet. Chem.*, 1968, **11**, 601.
12 The diameters and shell thicknesses of 120 and 40 particles were measured respectively.
13 J. F. Moulder, W. F. Stickle, P. E. Sobol and K. D. Bomben, *Handbook of X-ray Photoelectron Spectroscopy*, Physical Electronics, Inc., 1992.
14 The standard reduction potentials of Co^{2+} and Sn^{2+} are −0.28 V and −0.14 V respectively.
15 According to EDS and XPS analysis, **US-HS** contains 20% CoO (theoretical capacity: 716 mA h g^{-1}, ref. 3*b*). The theoretical maximum capacity of **US-HS** can be estimated to be 937 mA h g^{-1}.
16 In comparison, the SnCo(1 : 1)O_x materials obtained after 30 min and **US-HS** maintained 745 mA h g^{-1} and 947 mA h g^{-1} discharge capacities after 10 cycles, respectively.